



S. cerevisiae whole-cell based capacitive biochip for the detection of toxicity of different forms of carbon nanotubes



Ashish Pandey^{a,b}, Raghuraj S. Chouhan^b, Yasar Gurbuz^a, Javed H. Niazi^{b,*}, Anjum Qureshi^{b,**}

^a Faculty of Engineering and Natural Sciences, Sabanci University, Orhanli 34956, Istanbul, Turkey

^b Sabanci University Nanotechnology Research and Application Center Istanbul, Orta Mah. 34956, Istanbul, Turkey

ARTICLE INFO

Article history:

Received 4 March 2015

Received in revised form 4 May 2015

Accepted 6 May 2015

Available online 14 May 2015

Keywords:

Capacitive biochip

Whole-cells-on-chip

CNTs

SEM

Nanotoxicity

ABSTRACT

A whole-cell based capacitive biochip (WCB) was employed for detecting nanotoxicity of different types of carbon nanotubes (CNTs). The WCB was made of arrays of capacitors that were functionalized with living *S. cerevisiae* (yeast) cells through coupling on their cell-surface protein disulfide bridges. Cells-on-chip were exposed to varying concentrations of single-walled (SW), multi-walled (MW) and double-walled (DW) CNTs. Dynamic cell-surface charge distributions as a result of cell-CNT interactions on chip were measured as change in relative capacitance under the applied AC-frequency. The WCB response provided a direct relationship between the integrity of cells-on-chip and their strong interaction with CNTs by adsorption/adhesion. Cellular damages imposed by CNTs was determined based on the magnitude of changes in relative capacitance against different types and concentrations of CNTs. Increasing toxicity experienced by cells-on-chip followed the order DWCNTs < MWCNTs < SWCNTs suggesting that cells were severely affected by SWCNTs followed by MWCNTs and DWCNTs. The above results were further validated through cell viability tests and fluorescence assays using quantum dot conjugated cells that enabled determination of the responses at the interface of cell-membranes against different types of CNTs. The developed WCB can be extended to high-throughput screening of toxic nanomaterials (NMs) in food and environmental samples.

© 2015 Elsevier B.V. All rights reserved.

1. Introduction

Currently, over 500 consumer products in the market claim to contain elements of nanoscience and nanotechnology with daily new entries [1]. This market annually requires metric tons of raw NMs, ranging from nano-sized metals and metal oxide particles to CNTs [2,3]. The demand for nanotechnology in medical products was predicted to be around \$18 billion in 2014 [1]. CNTs are unique engineered nanomaterials (ENMs) as they possess enhanced physico-chemical properties, such as mechanical, thermal, or electrical conductivity that has attracted a great deal of research interest for many potential applications [4]. CNTs and other ENMs are produced in tons for incorporation in diverse commercial products ranging from rechargeable batteries, automotive parts and sporting goods to boat hulls and water filters [4].

Ever-increasing demand and utilization of these NMs ultimately emerge as multiple different sources of their disposal into the environment, eco-system, water or food supplies, or they find other routes of non-voluntary entry into the human body [3,5]. Therefore, toxicity and risk assessments of ENMs have received much attention. Currently, a complete understanding of the interactions of nanostructures with biological systems is lacking and thus it is unclear whether the exposure of nanostructures could produce harmful biological responses.

Yeast can be an ideal choice as biological sensing element to understand the harmful effects because of their rapid growth and response to external stress (stimuli), such as by toxic ENMs that may lead to altered cellular dynamics, including metabolism, growth and cell surface charge distribution. Such responses can be utilized to predict the toxicity impacts of chemicals on other living cells [6,7]. The toxicity response of cells is often determined in terms of stress responses imposed by chemicals, such as CNTs. The stress responses in cells primarily begin at the cell-surface, cell-wall or membrane. However, the results from cytotoxicity studies with CNTs and other NMs are often contradictory, mainly because of the use of different forms, sizes and functionalization of CNTs [8].

* Corresponding author. Tel.: +90 216 483 9879.

** Corresponding author. Tel.: +90 216 483 9000x2441; fax: +90 216 483 9885.

E-mail addresses: javed@sabanciuniv.edu, javedkolkar@gmail.com (J.H. Niazi), anjum@sabanciuniv.edu (A. Qureshi).

Additionally, use of different cell culture media [9] and a variety of different cell types contributed to the complexity of CNTs' toxicity [10]. Such observations underscore the need for simple methods to test toxicity of NMs on living cells [11].

To date, most traditional biological methods for *in vitro* and *in vivo* toxicological studies of CNTs and other ENMs on microbial cells are based on cellular activity and proliferations. These methods include growth and viability assays [12,13], proteomic assays, reactive oxygen species (ROS) detection tests [14,15] and molecular-level evaluations based on genetic responses [16,17]. Among all of the above methods, *in vitro* cytotoxicity methods are currently employed, which required labeling with fluorescent molecules for detection. These methods are used as markers for cell-viability and consist of procedures that provide results only at a final time-point [18]. The existing conventional analytical techniques reported in the literature usually require a lengthy and time-consuming process and often produce false positive results. Hence, there is a demand for a rapid, sensitive and accurate method for assessing toxicity in cells. Recently, due to the advantages of automation of fluids and minimization of human errors, integration of a cells-on-a-chip (CoC) system is gaining importance for nanotoxicity assessments. Micro-chip-based biosensors show a promising future for monitoring cellular nanotoxicity as they allow rapid, real-time and multi-sample analysis creating a versatile, noninvasive tool that is able to provide quantitative information with respect to alteration in cellular function upon exposure to various NMs' [19].

In recent experiments, chip-based electrochemical approach was used to test the toxicity of ENMs. These approaches were based on differential pulse voltammetry and electrical impedance sensing (EIS) method [20–23]. EIS based whole-cell sensor reported assessment of NMs' toxicity such as Au, Ag, CdO NPs and SWCNTs on human lung fibroblasts (CCL-153) and rainbow trout gill epithelial cells (RTgill-W1) [22]. All reported CoC-based approaches for nanotoxicity assessment utilized Faradaic-electrochemical principle that requires a redox mediator/chemical reagent to generate detectable signal which often leads to undesirable quenching effects with NPs.

In this study, we designed a label-free and reagent-free WCB chip based on non-Faradic electro-chemical impedance spectroscopy (nFEIS) method. WCB was successfully used to probe the size and concentration dependent toxicity of SWCNTs, DWCNTs and MWCNTs as NMs models. The developed WCB capacitive response was measured before and after the interaction of each type of CNTs with cells on chip under applied AC frequency. The WCB chip responses were validated through fluoresce based assay and cell viability measurements as a proof of concept.

2. Materials and methods

2.1. Chemicals and reagents

A wild type *S. cerevisiae* (BY-4741) (yeast) strain was used as a model living cell in this study. Yeast extract, peptone, dextrose broth/agar (YPD) media were purchased from Difco (MI, USA). Phosphate-buffered saline (PBS), 3-mercaptopropionic acid (MPA), 1-ethyl-3-[3-dimethylaminopropyl] carbodiimide hydrochloride (EDC) and *N*-hydroxysuccinimide (NHS), cysteamine, and tris(2-carboxyethyl)phosphine (TCEP) were purchased from Sigma-Aldrich, Germany. SWCNTs (outer diameter, O.D. \times length, $L=1\text{--}2\text{ nm}$, $5\text{--}20\text{ }\mu\text{m}$) and MWCNTs (O.D. \times $L=10\text{--}20\text{ nm}$, $5\text{--}30\text{ }\mu\text{m}$) were purchased from Arry®, Hong Kong. DWCNTs (O.D. \times $L=5\text{ nm}$ \times $50\text{ }\mu\text{m}$) were purchased from Sigma-Aldrich, USA. Triton-X 100 was procured from Merck, Germany. Qdot® 625 ITK™ carboxyl quantum dots having emission at 625 nm

with a blue light excitation were purchased from Invitrogen Co. (Dynabeads) and used as fluorescent tags.

2.2. Fabrication of capacitor array chip

An array of gold interdigitated microelectrode based capacitors was patterned on SiO₂ wafers (p-type, 0–100 Ω cm resistivity, (100) orientation; University Wafers, USA) using standard photolithography. The wafer was cleaned thoroughly with isopropanol, acetone and water simultaneously and then dried with N₂ gas. AZ5214E photoresist was layered on the wafer and image reversal was carried out using mask aligner and then it was baked at 120 °C for five min. For better adhesion of gold, a 50–60 nm thin titanium layer was first deposited on the wafer followed by deposition of 200–210 nm thick layer of gold using direct current sputter deposition. The deposition was carried out in presence of argon gas with power of 150 W for 3 min. The dimension of each electrode was measured to be 800 μm in length and 40 μm in width with a distance between two electrodes of 25 μm. Each wafer contained 45 independent capacitors in arrays each made of 24 gold microelectrodes within a total area of 3 mm².

2.3. *S. cerevisiae* cells culture preparation and cell surface activation

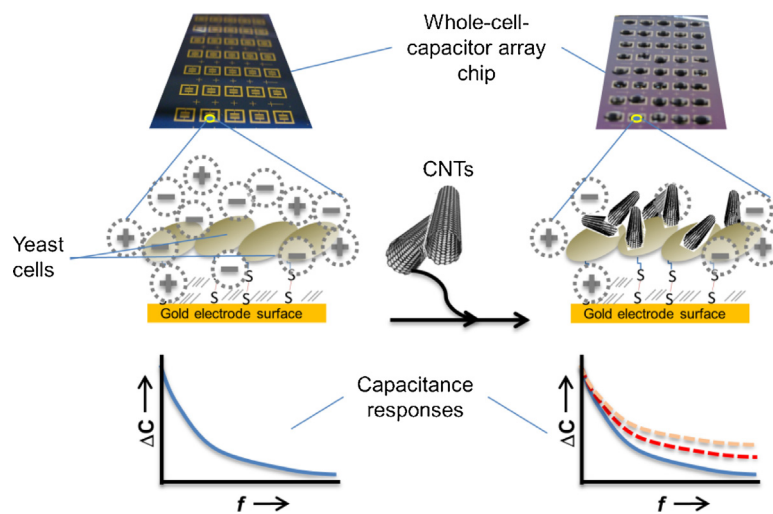
Wild type *S. cerevisiae* cells were cultured in YPD-broth at 30 °C for 18–20 h and then the cells were harvested by centrifugation at 5000 rpm for 1 min. The preparation of cell culture and surface-activation of capacitor chips with free –SH groups was used as reported in the literature [24] and the detailed information is given in SI.

2.4. Surface chemistry and immobilization of cells

The fabricated capacitor array was subjected to plasma cleaning followed by thorough washing with ethanol and finally dried with N₂ gas. To immobilize the TCEP treated yeast cells on capacitor chip, first the chip was immersed in 20 mM of ethanolic 3-mercaptopropionic acid (MPA) and incubated overnight at room temperature. After SAM formation, the chip was washed 2–3 times with water and dried using N₂ gas. The chips were then incubated with a mixture of 100 mM 1-ethyl-3-[3-dimethylaminopropyl] carbodiimide hydrochloride (EDC) and 50 mM of *N*-hydroxysuccinimide (NHS) and 50 mM of cysteamine for 3 h and thoroughly washed with distilled water. The surface-activated capacitor chips with free –SH groups were then incubated with –SH groups of TCEP treated yeast cells (10^7 CFU/ml). The whole yeast cells-immobilized-on-chips were used to study the effect of size and concentrations of single, double and multi-walled CNTs.

2.5. Exposure of CNTs (SWCNT, DWCNT and MWCNT) to cells on WCB

All three types of CNTs were suspended in freshly prepared PBS solution in presence of 0.01% Triton-X to obtain a homogeneous suspension of CNTs. Different forms of CNTs at varying concentrations from 0.1 ng/ml to 10 μg/ml (0.15, 0.61, 2.44, 9.77, 39.06, 156.25, 625, 2500, and 10,000 ng/ml) were incubated on capacitor chip. PBS solution containing only 0.01% Triton-X was used as control. The entire sensing area (3 mm²) immobilized with yeast cells was incubated with a series of concentrations of CNTs as indicated above in 5 μl volumes for 1 h at room temperature. After incubation, the capacitor chips were washed immediately with PBS solution and dried using a N₂ gun before measuring the dielectric properties.



Scheme 1. Schematic of WCB for detecting cytotoxicity of CNTs.

2.6. WCB response measurement (impedance/capacitance)

The impedance/capacitance responses of WCB were measured before and after the exposure of CNTs and compared with control by nFEIS. The capacitance/impedance responses were measured after each step of processing as follows: (1) bare chips (to validate the functionality of each capacitor), (2) chips immobilized with yeast cells, (3) after exposure of cells on chip with varying concentrations/types of CNTs and (4) heat-killed cells on chip which was used as a negative control. To measure the change in capacitance a Network Analyzer (Karl-Suss PM-5 RF Probe Station and Agilent-8720ES), was used after pre-calibrating using SOLT (short-open-load-through) method. A frequency range of 100–300 MHz was applied to measure the capacitance/impedance values and the data was exported to MATLAB® program for normalization and analysis using Eq. (1) as described previously [25].

$$\frac{C - C_0}{C_0} \times 100 \quad (1)$$

where C is the actual capacitance after the interaction of CNTs with yeast cells at a particular concentration and C_0 is the capacitance before interaction. A negative control experiment was conducted using capacitor chip containing heat-killed yeast cells. For this, chip immobilized with yeast cells (8×10^7 CFU/ml) were subjected to heat treatment in an air-tight and pre-heated humid chamber at 95 °C for 5 min followed by quickly freezing at −70 °C for 5 min and thawed at 25 °C for 15 min. The above treatment process was repeated thrice and finally the chip was dried using N₂ gas before taking measurements as negative controls. Technical and biological replicates ($n=3$) were determined and the percent relative standard deviations (%RSD) was calculated to be within 11%, and the standard deviations were shown as error bars in figures.

2.7. Bioconjugation of cells with QDs

Bioconjugation of yeast cells with quantum dot (QD₆₂₅) was carried out in two step reactions. (a) Free –COOH groups present on QDs were activated with cysteamine through covalent coupling to give rise to free –SH groups on QDs. (b) The free –SH groups of QDs were allowed to form disulphide bridges (–S–S–) on TCEP activated yeast cell surfaces. The details of preparation of bioconjugates were followed as reported previously from our laboratory [26].

2.8. Scanning electron and confocal microscopy

The morphological changes that occurred upon interaction of yeast cells with CNTs were examined by scanning electron microscopy (SEM) analysis (LEO Supra 35VP SEM). Confocal microscopy images of QD bioconjugated yeast were observed under a Carl-Zeiss LSM 710 confocal microscope with 405 nm laser excitation, and the images were collected by using a 553–718 nm filter.

2.9. Fluorescence and cell viability measurement of QD-bioconjugated cells before and after exposure of different forms of CNTs

Interaction of different forms of CNTs with cells was studied using QD-bioconjugated yeast and confirmed by: (a) measuring fluorescence emission from QD-bioconjugated cells and (b) viable cell count (CFU). The detailed experimental procedure is given in SI.

3. Results and discussion

In this study, we developed a whole-cell based capacitive biochip made of an array of interdigitated gold micro-electrodes forming capacitors (Scheme 1). Arrays of capacitors were activated by forming a SAM layer of MPA that extended free –COOH groups for immobilization. Surface activated yeast cells previously treated with TCEP to reduce cell surface –S–S– bridges were again activated by incubating with cysteamine. The –SH groups of cysteamine formed –S–S– bridges with –SH groups on TCEP treated yeast cells. The cysteamine arm on cell surfaces extended free –NH₂ groups that were utilized for covalent coupling of cells with –COOH groups of SAM layer on electrodes.

3.1. Density of cells interfaced on capacitor chip

Different cell concentrations of yeast cells (10^5 – 10^7 CFU) were immobilized on the capacitor chip to optimize the cell-density. The capacitor surfaces immobilized with yeast cells were examined by optical micrographs (Fig. 1a and b). We found that maximum cell adhesion took place at 10^7 CFU that showed densely packed structures of cells on surface area of the gold interdigitated electrode. The capacitive chip surface was further visualized under SEM to examine the intact morphology or architecture of the immobilized cells. Fig. 1c shows the SEM image of densely packed cells on electrodes that retained their native morphology and architecture.

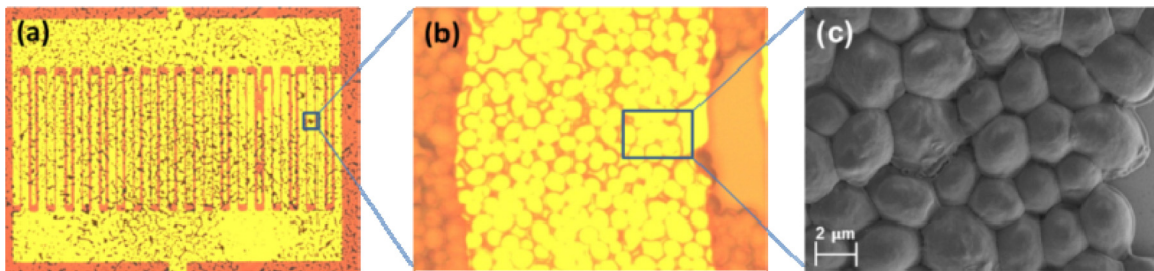


Fig. 1. Micrographs of WCB chip surface: (a) Optical image of MPA-SAM activated chips immobilized with yeast with concentrations of 8×10^7 cells, (b) a magnified portion of optical micrograph of an electrode and (c) SEM image of yeast cells immobilized on the surface of electrodes.

3.2. Response of WCB to CNTs (SWCNT, DWCNT and MWCNT)

Here, capacitance response of WCB was measured with respect to three different types of CNTs (SWCNT, DWCNT and MWCNT) at varying concentrations ranging 0.1 ng/ml to 10 μ g/ml. The electrical responses of WCB chip were examined by nFEIS against the applied frequency range of 100–300 MHz (Fig. 2a–c). A frequency of 200 MHz was chosen to elucidate distinct responses of WCB against different type/concentrations of CNTs (Fig. 2d). The relative capacitance response with respect to controls (only cells) and heat-killed cells (HKC) were analyzed as negative controls (Fig. 2d). The relative capacitive responses of yeast WCB was found to be dynamic with each type of CNTs such as SWCNT, DWCNT and MWCNT at different concentrations, respectively (Fig. 2a–c). The heat-killed cells on

chip however failed to respond to CNTs suggesting that the chip responses were originated from living activities of cells after their interactions with CNTs.

Relative capacitive response of WCB against SWCNTs was concentration dependent, ranging from 0.153 ng/ml up to 2500 ng/ml (Fig. 2a–d). However, WCB exposed with MWCNTs and DWCNTs exhibited response against maximum concentration of 625 ng/ml and beyond this the cells on WCB chip response attained saturation (Fig. 2b–d). Change in relative capacitance responses against CNTs could have occurred due to the toxicity imposed by CNTs on yeast cells on WCB chip. Therefore, it is postulated that the principle behind the determination of toxicity induced by CNTs using WCB chip was based on changes in relative surface capacitance upon interaction of cells-on-chip with each type of CNTs at

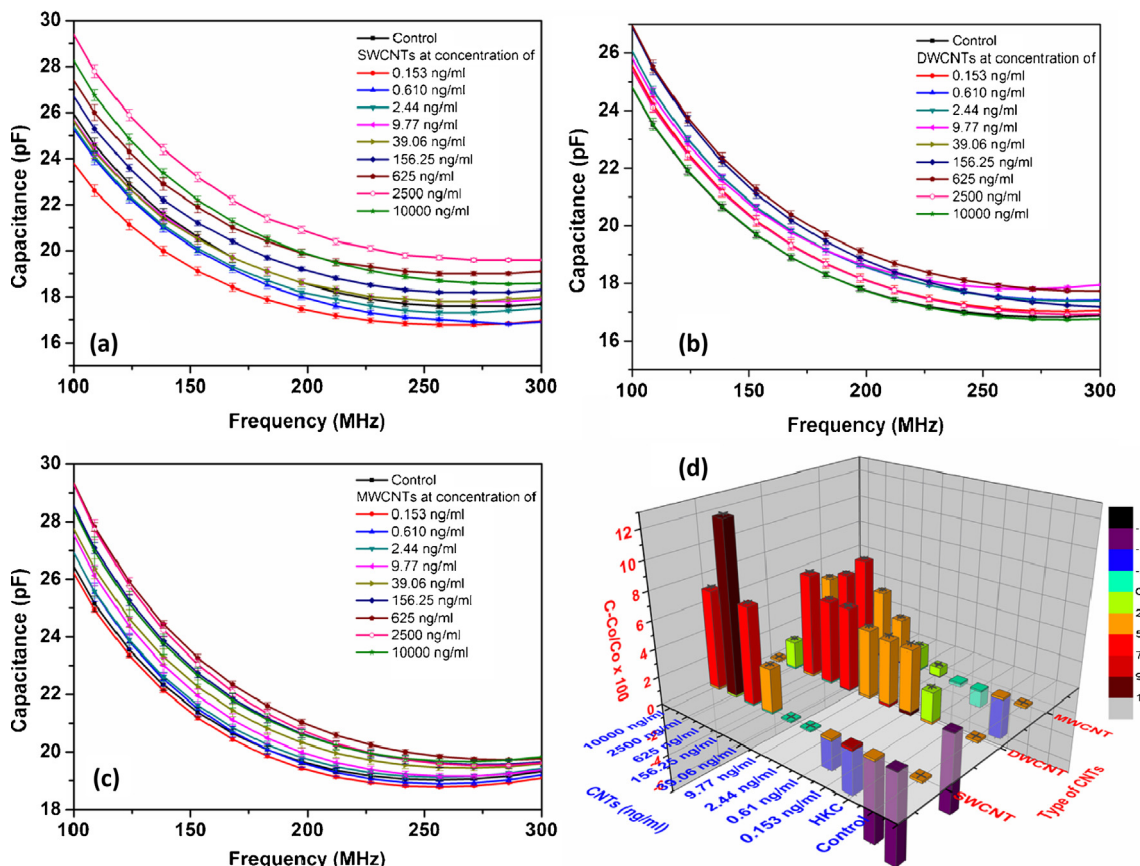


Fig. 2. Capacitance response profile with WCB chip as a function of applied frequency (100–300 MHz) when exposed to different concentrations of (a) SWCNTs, (b) DWCNTs and (c) MWCNTs and (d) 3D plot of relative capacitance responses derived from WCB responses against SWCNTs, DWCNTs and MWCNTs at different concentrations from 0.153 to 10,000 ng/ml at 200 MHz.

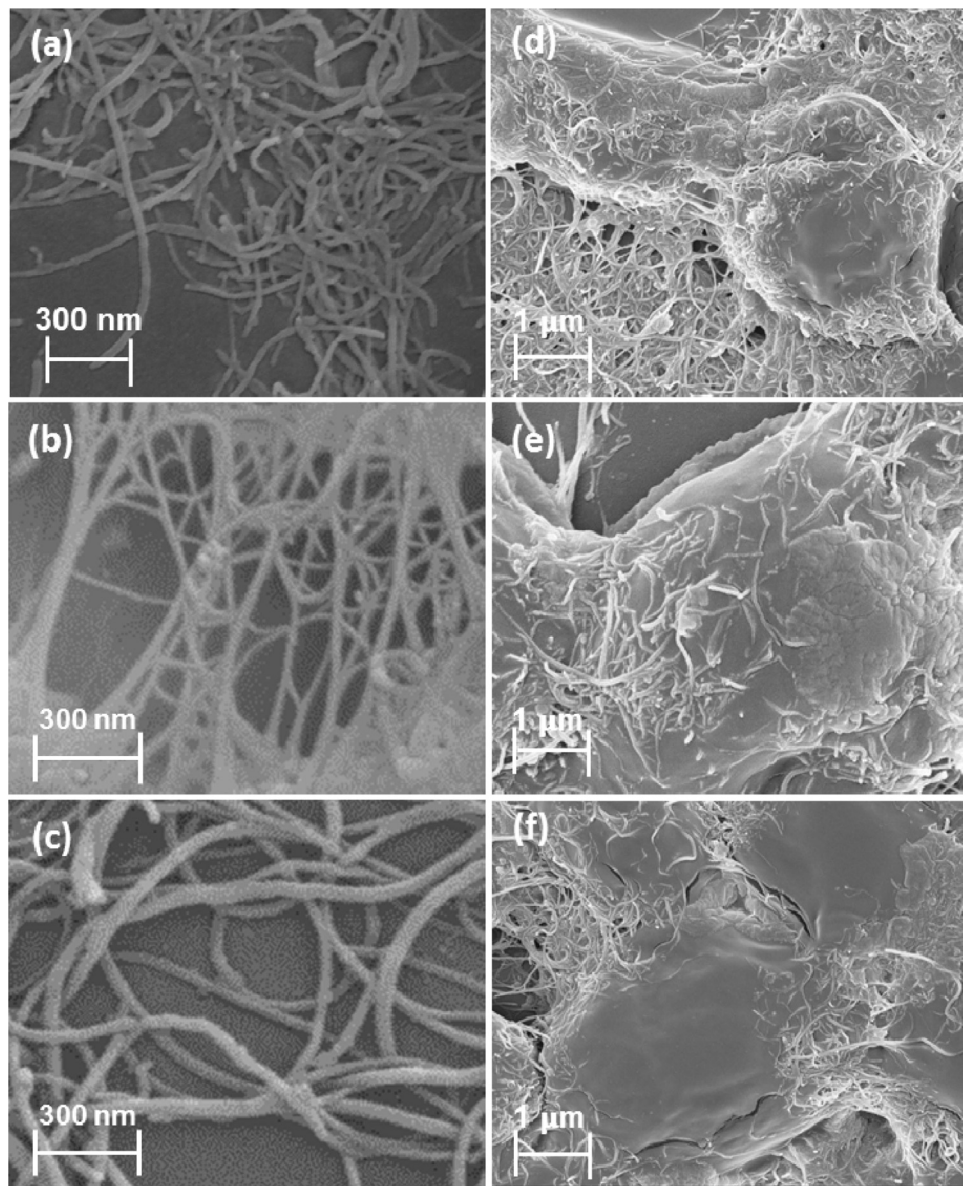


Fig. 3. SEM images of bare CNTs (a) SWCNTs (b) DWCNTs (c) MWCNTs, (d) yeast cells-on-WCB exposed with SWCNTs showing collapsed cell structure, (e) yeast cells-on-WCB exposed with DWCNTs showing intact cell structure and (f) yeast cells-on-WCB exposed with MWCNTs showing partial collapsed cell structure.

their respective concentrations. Interaction of cells with nanotubes induced damage to the cell membrane and thus resulted in change in capacitance response of chip.

Additionally, change in cell surface charges could also be explained in terms of polarization of cells surface charges before and after exposure of SWCNTs, DWCNTs and MWCNTs. Here, assuming that a complex cell structure is surrounded by positive and negative charges that arise from the ionizable side chains of the cell-surface protein structure [27]. The cumulative charges on chips can be measured in terms of a molecular dipole moment. Exposure of cells-on-WCB with different types of CNTs induce cellular stress conditions and as a result the outer membrane of the cells tend to rupture because of their physicochemical interactions with needle-like nanotubes, thus rendering an altered surface charge distribution [28]. Therefore, any perturbations such as those induced by different types of CNTs on cells would influence significant change in charge distribution that formed the basis for WCB responses.

The negative capacitance response observed in lower concentration of SWCNT may be attributed to the accumulation of electrical charges at the ends of SWCNT under an applied voltage (Fig. 2d) [29]. In a previous study, increase in concentration of nanotubes increases the van der Waal's forces which enabled SWCNTs to interact or pierce the yeast cells due to their needle like structures [26]. Other types of cells such as bacteria also possess a positive affinity to closely adhere to CNTs and get entrapped in a CNT network has also been previously observed [30]. In this study, the capacitive response with yeast cells-on-WCB upon their interaction with SWCNTs showed severe toxicity levels as compared with those found with yeast cells-on-WCB exposed with DWCNTs or MWCNTs (Fig. 2d). This could be attributed to one or more of the following reasons: (a) direct contact of cells with open ends of SWCNTs that might be a critical factor imparting more cytotoxicity and cause damage of cell membrane [31,32], (b) the electronic structure of SWCNTs also recently accounted for its antibacterial effects, where loss of cell viability is correlated

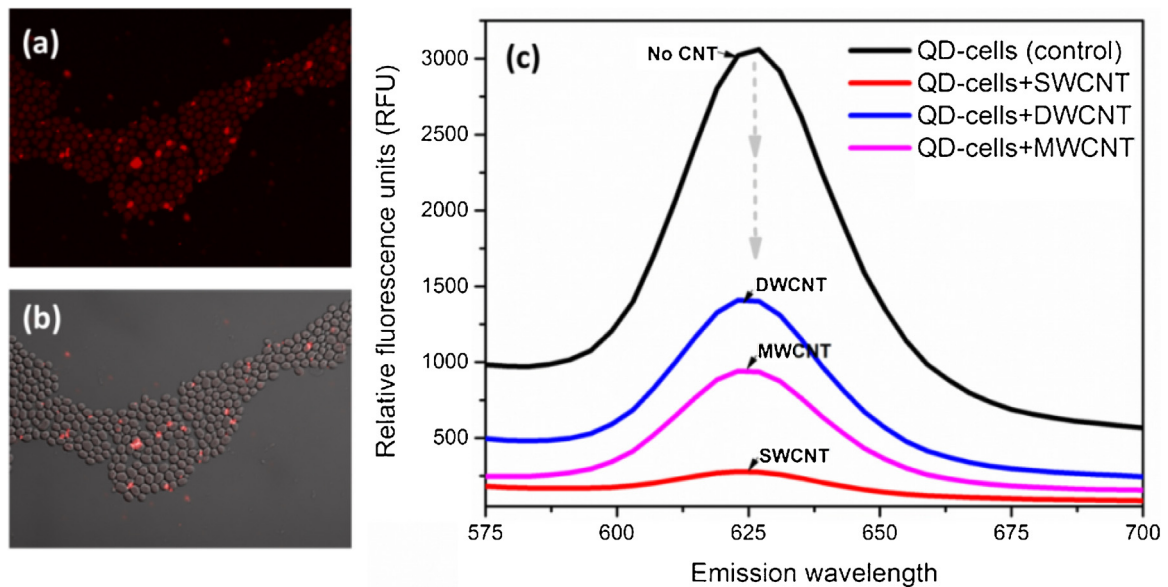


Fig. 4. (a) Confocal images of QD-bioconjugated yeast cells, (b) overlayed fluorescence and bright-field images of QD-cells and (c) fluorescence emission spectra of QD-yeast bioconjugates before and after exposure of 10 µg/ml of SWCNTs, DWCNTs and MWCNTs.

with metallic SWCNTs fractions [33] and/or (c) SWCNTs could also short-circuit the cells by forming a conductive bridge over the insulating bilayer of lipid and thereby discharging cellular energy to the external environment. Further, the WCB capacitance response was observed to increase with concentration of SWCNTs and MWCNTs, but this trend was not observed with DWCNTs (Fig. 2a–d). Since SWCNTs provided large surface area compared with other CNTs, the cells-on-WCB exposed to SWCNTs were therefore showing increase in capacitance responses. This result suggested that SWCNTs were more toxic when compared with DWCNTs and MWCNTs. Although, DWCNTs exhibited a moderate cytotoxicity with consistent or static responses with concentrations from 0.610 to 625 ng/ml, but it exhibited a least cytotoxicity amongst all three CNT types tested in this study. The mild cytotoxicity of DWCNTs could be attributed to the cell surface adhesion of DWCNTs which is consistent to previously reported studies [34]. On the other hand, capacitive response profiles of WCB against MWCNTs showed increased dynamic response up to 625 ng/ml concentration due to its stronger attraction with cells that also caused mild toxicity in cells or induce cellular damage by wrapping around the cell surface. It was reported that MWCNTs tends to be more flexible and thus allow formation of a mat-like structure around the cellular surface by wrapping and therefore cause mild osmotic stress to the cells [35]. Based on the magnitude of change in relative capacitance response using WCB against different type of CNTs, the increasing toxicity of CNTs was observed in the order of DWCNTs < MWCNTs < SWCNTs.

3.3. Morphological study

Interaction of various types of CNTs on the surface of yeast cells-on-WCB was examined by changes in cell morphology using SEM. SEM images of SWCNTs, DWCNTs and MWCNTs and cells after exposure of each type of CNTs (at 10 µg/ml) were acquired and shown in Fig. 3a–f. SEM images revealed that all three different types of CNTs were able to interact with the cells depending upon their affinity which directly related to physicochemical properties of each type of CNTs, such as the number of CNTs' walls (Fig. 3a–f). Loss of cellular integrity and deformation of outer membrane of the cells upon interaction with SWCNTs was clearly observed (Fig. 3a). The

SWCNTs perforated the cellular surface and induced mechanical damage on the cells (Fig. 3d). The cellular integrity was moderately affected by the interaction of cells with MWCNTs as seen in SEM (Fig. 3f), where MWCNTs appeared wrapped on the cell-wall and therefore inducing less toxicity as compared with SWCNTs with partial collapsed cell structure (Fig. 3f). However, DWCNTs did not affect the cells and thus allowing the cells to maintain their native structure (Fig. 3e). The above results are in good agreement with the result obtained from WCB chip (Fig. 2a–d) as well as those reported previously [26].

3.4. Fluorescence based assays and cell viability test and WCB validation

QD-bioconjugated yeast cells were used to determine the toxicity caused by each type of CNTs (SWCNT, DWCNT and MWCNT) to validate the WCB results. The QD-cells served as smart indicators upon close interaction of CNTs at the interface of cell-membrane that alter the fluorescence emission originating from cell-surface QDs. Fig. 4a and b shows the confocal fluorescence and bright-field images of QD-bioconjugated yeast cells. QD's emission was ascertained from confocal imaging that showed QDs were indeed coupled on yeast cell surfaces and causing no detrimental effects to the cells (Fig. 4a and b). The fluorescence emission spectra of QD-yeast bioconjugates were recorded before and after interaction with homogeneous suspension of 10 µg/ml concentrations of SWCNTs, DWCNTs and MWCNTs for 1 h. We here observed significant loss of fluorescence intensity upon exposure of QD-bioconjugated yeast cells with SWCNTs (Fig. 4c). However, a slight quenching of photoluminescence or reduced fluorescence intensity in QD-bioconjugated yeast cells occurred after exposure of DWCNTs and MWCNTs. The changes in fluorescence spectra signal upon exposure of each type of CNTs as well as cell viability results (Supporting Information Fig. S1) was consistent with WCB chip results, where SWCNTs exhibited significant change in fluorescence signal, greater reduction in cell viability (70%) and enhanced capacitance responses, respectively and thus validating that the developed WCB can be successfully used for detecting toxicity induced by CNTs.

4. Conclusion

In this study, a whole-cell based capacitive biochip was developed for detecting cytotoxicity induced by different forms of CNTs (SWCNT, DWCNT and MWCNT). This WCB utilized living yeast cells-on-chip to determine the detrimental effects of SWCNTs, DWCNTs and MWCNTs. The WCB response was highly sensitive to the type of CNTs and their concentrations. The dynamic response of each type of CNTs with WCB was shown to be dependent on their physicochemical properties, including number of walls present in CNTs. Thus, different forms of CNTs have different physicochemical characteristics that mainly influence on their sizes due to varying number of walls that significantly affect the living cells-on-chip (WCB). It was found that each type of CNTs has different extent of causing detrimental effects on cells' living activity based on their mode of interactions, such as piercing, adhesion or wrapping around the cells as has been observed by SEM. The WCB responses were found to be dependent on the type of CNTs and followed the decreasing order of toxicity of SWCNT > MWCNT > DWCNT suggesting that DWCNT was least toxic to cells. The WCB responses were further validated using fluorescence based assays and cell viability tests that were in good accordance with the developed WCB responses. Therefore, the developed WCB could offer a versatile tool for testing toxicities of nanostructures.

Acknowledgement

This work was supported by the Scientific and Technological Research Council of Turkey (TUBITAK), Project grant Nos. 112E051 for AQ and 112Y309 for JHN, and the authors thank for this support.

Appendix A. Supplementary data

Supplementary data associated with this article can be found, in the online version, at <http://dx.doi.org/10.1016/j.snb.2015.05.008>

References

- [1] C.F. Jones, D.W. Grainger, In vitro assessments of nanomaterial toxicity, *Adv. Drug Deliv. Rev.* 61 (2009) 438–456.
- [2] A.M. Thayer, Carbon nanotubes by the metric ton, *Chem. Eng. News Arch.* 85 (2007) 29–35.
- [3] W. Hannan, P.B. Thompson, Nanotechnology, risk and the environment: a review, *J. Environ. Monit.* 10 (2008) 291–300.
- [4] Y. Liu, Y. Zhao, B. Sun, C. Chen, Understanding the toxicity of carbon nanotubes, *Acc. Chem. Res.* 46 (2012) 702–713.
- [5] R.N. Seetharam, K.R. Sridhar, Nanotoxicity threat posed by nanoparticles, *Curr. Sci. India* 93 (2007) 769–770.
- [6] J.H. Lee, C.H. Youn, B.C. Kim, M.B. Gu, An oxidative stress-specific bacterial cell array chip for toxicity analysis, *Biosens. Bioelectron.* 22 (2007) 2223–2229.
- [7] J.L. Ramos, T. Krell, C. Daniels, A. Segura, E. Duque, Responses of *Pseudomonas* to small toxic molecules by a mosaic of domains, *Curr. Opin. Microbiol.* 12 (2009) 215–220.
- [8] P. Wick, P. Manser, L.K. Limbach, U. Dettlaff-Weglikowska, F. Krumeich, S. Roth, W.J. Stark, A. Bruinink, The degree and kind of agglomeration affect carbon nanotube cytotoxicity, *Toxicol. Lett.* 168 (2007) 121–131.
- [9] Y. Zhu, T.C. Ran, Y.G. Li, J.X. Guo, W.X. Li, Dependence of the cytotoxicity of multi-walled carbon nanotubes on the culture medium, *Nanotechnology* 17 (2006) 4668–4674.
- [10] K. Kostarelos, L. Lacerda, G. Pastorin, W. Wu, S. Wieckowski, J. Luangsivilay, S. Godfrey, D. Pantarotto, J.-P. Briand, S. Muller, M. Prato, A. Bianco, Cellular uptake of functionalized carbon nanotubes is independent of functional group and cell type, *Nat. Nano* 2 (2007) 108–113.
- [11] K.J. Boor, Bacterial stress responses: what doesn't kill them can make them stronger, *PLoS Biol.* 4 (2006) 18–20.
- [12] G. Oberdorster, E. Oberdorster, J. Oberdorster, Nanotoxicology: an emerging discipline evolving from studies of ultrafine particles, *Environ. Health Perspect.* 113 (2005) 823–839.
- [13] S. Chatterjee, A. Bandyopadhyay, K. Sarkar, Effect of iron oxide and gold nanoparticles on bacterial growth leading towards biological application, *J. Nanobiotechnol.* 9 (2011).
- [14] L. Brunet, D.Y. Lyon, E.M. Hotze, P.J. Alvarez, M.R. Wiesner, Comparative photoactivity and antibacterial properties of C60 fullerenes and titanium dioxide nanoparticles, *Environ. Sci. Technol.* 43 (2009) 4355–4360.
- [15] O. Choi, Z. Hu, Size dependent and reactive oxygen species related nanosilver toxicity to nitrifying bacteria, *Environ. Sci. Technol.* 42 (2008) 4583–4588.
- [16] Y.P. Xie, Y.P. He, P.L. Irwin, T. Jin, X.M. Shi, Antibacterial activity and mechanism of action of zinc oxide nanoparticles against *Campylobacter jejuni*, *Appl. Environ. Microbiol.* 77 (2011) 2325–2331.
- [17] J.S. McQuillan, A.M. Shaw, Whole-cell *Escherichia coli*-based bio-sensor assay for dual zinc oxide nanoparticle toxicity mechanisms, *Biosens. Bioelectron.* 51 (2014) 274–279.
- [18] S.M. Hussain, K.L. Hess, J.M. Gearhart, K.T. Geiss, J.J. Schlager, In vitro toxicity of nanoparticles in BRL 3A rat liver cells, *Toxicol. In Vitro* 19 (2005) 975–983.
- [19] G. Velve-Casquillas, M. Le Berre, M. Piel, P.T. Tran, Microfluidic tools for cell biological research, *Nano Today* 5 (2010) 28–47.
- [20] D. Kim, Y.-S. Lin, C.L. Haynes, On-chip evaluation of shear stress effect on cytotoxicity of mesoporous silica nanoparticles, *Anal. Chem.* 83 (2011) 8377–8382.
- [21] T.H. Kim, S.R. Kang, B.K. Oh, J.W. Choi, Cell chip for detection of silica nanoparticle-induced cytotoxicity, *Sens. Lett.* 9 (2011) 861–865.
- [22] E. Hondroulis, C. Liu, C.Z. Li, Whole cell based electrical impedance sensing approach for a rapid nanotoxicity assay, *Nanotechnology* 21 (2010).
- [23] F.A. Alexander Jr., E.G. Huey, D.T. Price, S. Bhansali, Real-time impedance analysis of silica nanowire toxicity on epithelial breast cancer cells, *Analyst* 137 (2012) 5823–5828.
- [24] X. Shi, G.E. Garcia, R.J. Neill, R.K. Gordon, TCEP treatment reduces proteolytic activity of BoNT/B in human neuronal SHSY-5Y cells, *J. Cell. Biochem.* 107 (2009) 1021–1030.
- [25] E.A. de Vasconcelos, N.G. Peres, C.O. Pereira, V.L. da Silva, Potential of a simplified measurement scheme and device structure for a low cost label-free point-of-care capacitive biosensor, *Biosens. Bioelectron.* 25 (2009) 870–876.
- [26] R.S. Chouhan, A. Qureshi, J.H. Niazi, Quantum dot conjugated *S. cerevisiae* as smart nanotoxicity indicators for screening the toxicity of nanomaterials, *J. Mater. Chem. B* 2 (2014) 3618–3625.
- [27] J.S. Dickson, M. Koohmaraie, Cell surface charge characteristics and their relationship to bacterial attachment to meat surfaces, *Appl. Environ. Microbiol.* 55 (1989) 832–836.
- [28] N. Narayanan, C.P. Chou, Physiological improvement to enhance *Escherichia coli* cell-surface display via reducing extracytoplasmic stress, *Biotechnol. Prog.* 24 (2008) 293–301.
- [29] P. Kebinski, S. Nayak, P. Zapols, P. Ajayan, Charge distribution and stability of charged carbon nanotubes, *Phys. Rev. Lett.* 89 (2002) 255503.
- [30] T. Akasaka, F. Watari, Capture of bacteria by flexible carbon nanotubes, *Acta Biomater.* 5 (2009) 607–612.
- [31] S. Kang, M. Pinault, L.D. Pfefferle, M. Elimelech, Single-walled carbon nanotubes exhibit strong antimicrobial activity, *Langmuir* 23 (2007) 8670–8673.
- [32] S. Kang, M. Herzberg, D.F. Rodrigues, M. Elimelech, Antibacterial effects of carbon nanotubes: size does matter!, *Langmuir* 24 (2008) 6409–6413.
- [33] C.D. Vecitis, K.R. Zodrow, S. Kang, M. Elimelech, Electronic-structure-dependent bacterial cytotoxicity of single-walled carbon nanotubes, *ACS Nano* 4 (2010) 5471–5479.
- [34] O.N. Ruiz, K.S. Fernando, B. Wang, N.A. Brown, P.G. Luo, N.D. McNamara, M. Vangness, Y.-P. Sun, C.E. Bunker, Graphene oxide: a nonspecific enhancer of cellular growth, *ACS Nano* 5 (2011) 8100–8107.
- [35] H. Chen, B. Wang, D. Gao, M. Guan, L. Zheng, H. Ouyang, Z. Chai, Y. Zhao, W. Feng, Broad-spectrum antibacterial activity of carbon nanotubes to human gut bacteria, *Small* 9 (2013) 2735–2746.

Biographies

Ashish Pandey received his master degree in nanotechnology from MS University of Baroda, India. He is currently doing PhD in material science and engineering programme at Sabanci University, Istanbul, Turkey.

Dr. Raghuraj S. Chouhan received his PhD degree in biotechnology from Mysore University, India in 2011, and now working as a postdoctoral fellow at Sabanci University Nanotechnology Research and Application Centre, Turkey. His research areas include biosensor platforms for different analytes, cytotoxicity of nanomaterials, and biodevices for the biomedical applications.

Prof. Yasar Gurbuz received his B.Sc. degree in electronics engineering in 1990 from Erciyes University in Turkey, M.Sc. degree in 1993 and PhD degree in 1997 in electrical engineering from Vanderbilt University in the USA. He worked as a senior research associate at Vanderbilt between 1997 and 1999. From 1999 to 2000 he worked at Aselsan Inc. He joined Sabanci University in 2000 as a faculty member in the Faculty of Engineering and Natural Sciences, where he is currently a full professor. His research areas include RF/Analog/Mixed-Signal Integrated Circuits, solid-state devices and sensors, and microelectromechanical systems (MEMS). He is a member of IEEE and SPIE.

Dr. Javed H. Niazi received his PhD degree in biochemistry in 2003 from Gulbarga University, India. He worked as postdoctoral fellow and later visiting scientist from 2004 to 2006 at Gwangju Institute of Science & Technology and Korea Institute of Science & Technology, South Korea. Later he continued his research as a postdoctoral researcher turned Research Professor at School of Life Sciences and Biotechnology, Korea University, South Korea during 2007–2009. He joined Faculty of Engineering & Natural Sciences at Sabanci University as a visiting faculty, and currently working

as Senior Researcher at Sabanci University Nanotechnology Research & Application Center (SUNUM), Turkey. His research areas include: (a) *In vitro* selection and modification of synthetic ssDNA/RNA aptamers as affinity ligands for disease biomarkers and drugs; (b) aptamer-facilitated biomarker discovery; (c) design and development of novel assays for biosensor applications-mainly for cardiovascular and cancer diseases and (d) nanotoxicology.

Dr. Anjum Qureshi received her PhD degree in physics in 2008 from MS University of Baroda, India. She is currently working as a research faculty at Sabanci University Nanotechnology Research & Application Center, Turkey. Her research interests include studying physics of biological systems, detection of cardiac/cancer diseases biomarkers by electrochemical biosensors and modification of polymer nano-composites and nanomaterials by irradiation.